Hydrol. Earth Syst. Sci. Discuss., 12, 2435–2476, 2015
www.hydrol-earth-syst-sci-discuss.net/12/2435/2015/
doi:10.5194/hessd-12-2435-2015
© Author(s) 2015. CC Attribution 3.0 License.

Hydrology and Earth System Sciences
Open Access
Discussions

This discussion paper is/has been under review for the journal Hydrology and Earth System Sciences (HESS). Please refer to the corresponding final paper in HESS if available.

Vulnerability of groundwater resources to interaction with river water in a boreal catchment

A. Rautio[1], A.-L. Kivimäki[2], K. Korkka-Niemi[1], M. Nygård[3], V.-P. Salonen[1], K. Lahti[2], and H. Vahtera[2]

[1]Department of Geosciences and Geography, University of Helsinki, Helsinki, Finland
[2]Water Protection Association of the River Vantaa and Helsinki Region, Helsinki, Finland
[3]Pöyry Finland Oy, Vantaa Water & Environment P.O. Box 50, Vantaa, Finland

Received: 24 December 2014 – Accepted: 3 February 2015 – Published: 25 February 2015

Correspondence to: A. Rautio (anne.rautio@helsinki.fi)

Published by Copernicus Publications on behalf of the European Geosciences Union.

Abstract

A low altitude aerial infrared (AIR) survey was conducted to identify hydraulic connections between aquifers and rivers, and to map spatial surface temperature patterns along boreal rivers. In addition, the stable isotopic compositions (δ^{18}O, δD), dissolved silica (DSi) concentrations and electrical conductivity of water in combination with AIR data were used as tracers to verify the observed groundwater discharge into the river system in a boreal catchment. The results of AIR surveys and hydrogeochemical studies performed in the boreal catchment are presented. Based on low temperature anomalies in the AIR survey, around 370 groundwater–surface water interaction sites were located along the main river channel and its tributaries (203 km altogether). On the basis of AIR survey, the longitudinal temperature patterns of the studied rivers differed noticeably. The stable isotopes and DSi composition revealed major differences between the studied rivers. The interaction locations identified in the proximity of 12 municipal water intake plants during the low-flow seasons should be considered as potential risk areas for water intake plants during flood periods (groundwater quality deterioration due to bank infiltration), and should be taken under consideration in river basin management under changing climatic situations.

1 Introduction

Interactions between groundwater (GW) and surface water (SW) are complex, and the rates of exchange are spatio-temporally highly variable (Tóth, 1963; Winter et al., 1998), depending on shoreline and river-bed sediments, aquifer characteristics, topography and meteorological conditions (Sebestyen and Schneider, 2001; Schneider et al., 2005; Rosenberry and LaBaugh, 2008). River channel interactions can be classified as gaining, losing, parallel flow and flow-through (Winter, 1998; Woessner, 1998) and they can vary through time within a year (Winter, 1998). Evidently, GW has an important role in maintaining stream flow, thermal buffering, water quality and beneficial habitat for fish

HESSD
12, 2435–2476, 2015

and freshwater aquatic life in rivers (Hansen, 1975; Stanford and Ward, 1993; Brunke and Gonser, 1997; Boulton et al., 1998; Woessner, 2000; Loheide and Gorelick, 2006).

Large fluctuations in the river flow rate, the low percentage cover of lakes, the high relative percentage of headwater lakes, the flat topography and generally poor infiltration rate of the soils are related to the relatively high flooding sensitivity of the studied catchment in southern Finland (Mäntylä and Saarelainen, 2008) (Fig. 1). Furthermore, the continuous development and construction of new areas in the densely populated capital region has increased the flood risk during peak flow periods (Suhonen and Rantakokko, 2006) (Fig. 2a). This has been acknowledged in a number of recent surveys in which riparian areas vulnerable to floods in the studied river catchment have been identified (i.a. Mäntylä and Saarelainen, 2008). Climate change is predicted to result in increasing annual precipitation and elevated temperatures during the twenty-first century (Jylhä et al., 2004), as well as an expected intensification of extreme precipitation events (Beniston et al., 2007), which will significantly increase the flooding risk in some southern Finnish watersheds according to Veijalainen et al. (2010). Frequency of summer floods due to the extreme precipitation and winter floods due to mild winters are expected to increase in the tributaries of the River Vantaa (Veijalainen et al., 2009). The statistical analysis of frequency and intensity of floods in Finland during the last 50 years reveals that frequency of winter floods has already increased throughout the country. In northern Finland floods mainly occur in December whereas in southern Finland floods can be witnessed all through winter months (Kuusisto, 2015).

The water quality of the River Vantaa and its tributaries has regularly been monitored since the 1970s in order to identify the incoming load of nutrients and contaminants. In the River Vantaa catchment, the river water (RW) has generally high nutrient concentrations and poor hygienic quality during heavy rains and the spring thaw (Vahtera et al., 2014). Flooding and heavy rain have the potential to induce contamination of municipal water intake wells via both overland flows entering the wells and by RW bank infiltration into the aquifer. There are twenty eight GW intake plants in the studied drainage basin, 12 of which are located in the proximity of main stream channels and are poten-

HESSD
12, 2435–2476, 2015

tially vulnerable to RW contamination during high peak flow (Fig. 1a). A summer flood in 2004 resulted in water quality problems at two major GW intake plants (Suhonen and Rantakokko, 2006), as well as the contamination of several GW wells (Silander et al., 2006) in the studied river catchment. In the River Vantaa drainage basin, there is a need for more comprehensive understanding of GW–SW exchange processes with respect to the water supply, water quality and characteristics of the aquatic environment under changing climatic conditions. The GW–RW exchange zones may have a more significant impact on water quality and quantity in the River Vantaa and its tributaries than has thus far been acknowledged.

The assumption is that GW–RW exchange can possibly be an important factor affecting the quality of water in municipal water intake plants, where a hydraulic connection between the river and the aquifer exists. The main aim of this study was to gain a better understanding of aquifer–river channel interaction and the potential vulnerability of municipal water intake plants in the studied catchment. This will also improve the general understanding of GW–SW interactions in the boreal catchments under changing climatic conditions, potentially affecting quality of groundwater utilized by waterworks. A low altitude survey (AIR) survey was carried out to identify areas of thermal anomalies as potential GW discharge locations to river beds, based on the temperature contrast between RW and GW (e.g. Torgersen et al., 2001; Loheide and Gorelick, 2006; Davis, 2007; Conant and Mochnacz, 2009; Loheide and Deitchman, 2009) and to produce spatially continuous temperature profiles of the surveyed rivers. More detailed field studies were performed at study sites in the Rivers Vantaa and Palojoki (Fig. 2b). Moreover, the stable isotopic compositions (δ^{18}O, δD), as well as dissolved silica (DSi) concentrations of GW and RW were used as tracers to verify the observed GW discharge into the river system. The additional objective was to assess the applicability of thermal and hydrogeochemical methods in defining the most vulnerable locations.

HESSD
12, 2435–2476, 2015

2 Study area

The River Vantaa is one of the water reserves for Finland's capital region (ca. 1 million inhabitants). The total catchment area of the River Vantaa is 1685 km^2 and the percentage cover of lakes is 2.25 % (Fig. 1a), the largest lake having a total area of 6.0 km^2 (Seuna, 1971; Ekholm, 1993). The length of the River Vantaa is 99 km, while its tributaries range in length from 8 to 65 km (Tikkanen, 1989) (Table 1). The surveyed rivers were slow to moderate flowing streams in a gently undulating glacial landscape that ranged in elevation from 20 to 120 m a.s.l. The surveyed rivers contained straight and meandering channel types.

River Vantaa catchment is characterized by strong snow-dominated seasonality, and major floods can be caused by either snowmelt or heavy rain events (Veijalainen et al., 2010). The highest flow rates typically occur during the spring and late autumn months due to snow melt (spring thaw) and heavy rains in autumns. The mean annual precipitation at the nearest weather stations, Vantaa (Helsinki-Vantaa airport) and Hyvinkää (Hyvinkäänkylä), is 682 and 660 mm, respectively (Pirinen et al., 2012) (Fig. 2b). Approximately 10–20 % of the precipitation falls as snow in southern Finland (Karlsson, 1986). The mean annual air temperature varies from 4.1 to 5.0 °C in the study area (Finnish Meteorological Institute, 1991).

In the northern part of the study area, the elevation ranges from +100 to +160 m a.s.l. (Fig. 1b), and the dominant geomorphological relief types are bedrock terrain and glacigenic deposits forming cover-moraine sheets and end-moraine ridges (Tikkanen, 1989) (Fig. 1a). The elevation decreases relatively smoothly towards the south, the majority of the central and southern parts of the catchment being lower than +80 m a.s.l. (Fig. 1b). In the lower areas, Quaternary deposits are dominated by marine and lacustrine silt and clay, which cover 39 % of the entire catchment area (Helsinki-Uusimaa Region, 1997). Riverbeds only sporadically overlap glaciofluvial sand and gravel formations (Fig. 1a), as they generally pass along bedrock fracture zones covered by thick clay layers (Tikkanen, 1989). Major GW reserves are associated with glaciofluvial es-

HESSD
12, 2435–2476, 2015

kers mainly hosting unconfined aquifers. However, semi-confined or confined parts of aquifers also occur in places (Table 1). Within the River Vantaa catchment, 29 aquifers in close vicinity to river beds are classified as important ones that are used by municipal water companies (Fig. 1).

Land use is divided between forestry 51 %, agriculture 26 % and urban (artificial surfaces) land use 20 % (Fig. 2a). Land use varies between the River Vantaa and its tributaries, as the headwater areas are dominated by forestry and southern areas by urban land use (Fig. 2a).

At field study sites in both the River Vantaa and River Palojoki, the river bed perpendicularly cuts glaciofluvial sandy esker ridge (Figs. 2b and 3). However, the bed of River Vantaa is steep sloped and bottom sediments mainly consist of loam with low permeability, whereas the bed of the shallow River Palojoki is gently sloped and bottom sediments consist of sand and gravel, enhancing GW discharge to the river through the river bottom.

The thickness of glaciofluvial material varies between 10 and 35 m under the Hyvinkäänkylä study site beside the River Vantaa, and GW in the aquifer flows towards the River Vantaa from both the north and south (Breilin et al., 2004) (Fig. 3a). The Hyvinkäänkylä water intake plant is located in close proximity to the north bank of the River Vantaa, and the three production wells are located 30–60 m from the River Vantaa channel (Fig. 3a).

At the study site in the River Palojoki, the river bed is significantly shallower and narrower than that of the River Vantaa (Table 1) and the sediments are composed of coarse-grained sand and gravel. The Tuusula artificial GW plant is located on the NW side of the River Palojoki channel, on the NWSE discontinuous Tuusula esker chain (Fig. 3b). The formation of natural GW in the shallow and unconfined Jäniksenlinna aquifer is approximately 4000 $m^3 d^{-1}$ (Hatva, 1989). Water from Lake Päijänne (9370 $m^3 d^{-1}$) is recharged into the aquifer by pond infiltration. GW flows towards the River Palojoki from the NW (mostly artificial GW) and SE (mostly natural GW) (Helmisaari et al., 2003) (Fig. 3b).

HESSD
12, 2435–2476, 2015

3 Methods

3.1 AIR surveys and field measurements

AIR has proved to be a feasible method for identifying GW–RW interaction in previous hydrological studies (e.g. Torgersen et al., 2001; Conant and Mochnacz, 2009). Furthermore, AIR provides a method for collecting spatially continuous patterns of river temperatures in an entire river over a short period of time (Faux et al., 2001; Torgersen et al., 2001; Cristea and Burges, 2009). In Finland, the conditions are most favourable for AIR studies from July to August, when the annual maximum contrast exists between GW (4–8 °C) and RW (20–24 °C) temperatures.

An AIR survey was conducted over the River Vantaa and its tributaries, Herajoki, Palojoki, Keravanjoki and Tuusulanjoki in July 2010 during the low-flow period (Fig. 2b). The technical details of the AIR survey in 2010 have been reported by Korkka-Niemi et al. (2012). July 2010 was warm and had low precipitation (15 mm, Finnish Meteorological Institute), apart from few thunderstorms.

In July 2011, an AIR survey was conducted over the Rivers Vantaa, Keravanjoki and Lepsämänjoki (Fig. 2b). Altogether, the AIR surveys covered 203 km of rivers as well as the riparian areas alongside the channels in 2010 and 2011 (Fig. 2b). Due to the preceding warm weather conditions, which prevailed for several weeks, the conditions were ideal for detecting GW discharge locations in summer 2011. A FLIR ThermaCAM P60 together with an HDR-CX700 digital video camera was used, with the cameras held in a near vertical position on the side of the helicopter. Thermal images were collected digitally and recorded from the sensor to the on-board computer at a rate of 5 frames s^{-1}, which guaranteed full overlap between the image frames. Digital image files were tagged with the acquisition time and with the position from a built-in GPS. The thermal and digital video cameras synchronized data collection to the nearest second and provided a means of correlating thermal and visible band imagery during postflight image processing.

HESSD
12, 2435–2476, 2015

Both thermal cameras used in AIR surveys had a pixel resolution of 320 × 240, a spectral range of 7.5–13 µm and a field of view of 24 × 18°. The FLIR system was capable of detecting temperature differences of ±0.08 °C with an accuracy of ±2.0 °C or ±2.0 % of the reading, as reported by the manufacturer.

Fine-scale adjustments of the flight path and altitude were made visually by the pilot in cooperation with the FLIR operator and attempted to capture both the rivers and a significant proportion of the riparian areas on side of the channels. Aerial surveys were mainly conducted in an upstream direction during the early afternoon hours in calm and cloudless weather conditions. Meteorological data on air temperature and relative humidity during the aerial surveys were obtained from the two nearest weather stations (Fig. 2b). The flight altitude of 100–300 m a.g.s. produced a ground resolution from 0.15 to 0.5 m. The ground speed varied between 50 and 90 km h^{-1}, depending on the stream width and intensity of meandering. Ground speed was maintained at 50 km h^{-1} over narrow, meandering streams and increased to 90 km h^{-1} over wide, straight rivers sections. The canopy cover from riparian vegetation ranged from nearly completely closed to wide open and varied within and between the rivers surveyed.

Reference measurements were collected simultaneously with AIR survey to compare the kinetic water temperature (T_k) measured 5 cm below the surface with a thermometer to the radiant water temperature (T_r) measured remotely with a thermal sensor in 2010 and 2011. The reference measurements were collected by discrete manual measurements with a YSI 600 XLM-V2-M multiparameter probe (accuracy ±0.15 °C) at River Keravanjoki study site in 2010 and the River Lepsämänjoki in 2011.

The T_r values were adjusted for the emissivity of natural water (0.96) and with inputs of air temperature, relative humidity and path length in post-processing. In producing the spatially continuous profiles of minimum radiant water temperature (T_{minr}), thermal images were individually analysed and T_{minr} was manually sampled from each thermal image of the main stream channel, and the lowest value for T_{minr} was selected for each second. T_{minr} was selected for this study to more efficiently localize the GW discharge and lower temperature zones in the main stream channel than with extraction methods

HESSD
12, 2435–2476, 2015

based on image sampling or weighted averages used in previous studies (Torgersen et al., 2001; Cristea and Burges, 2009). The thermal anomalies in the proximity of the main stream channel were examined and compared with the base map and visible band imagery to exclude artificial cold anomalies such as roads or electrical power lines.

Detailed field studies were performed at Hyvinkäänkylä and River Palojoki study sites in 2010 (Figs. 2b, 3 and Table 1). 19 cross-sections of the RW temperature and electrical conductivity (EC) near the sediment–water interface and sediment temperature at intervals of 1 to 2 m were measured at study sites representing different hydrogeological and hydrological settings. In addition, two longitudinal profiles of RW temperature near the sediment–water interface were collected. The RW temperature and EC measurements were collected with a YSI 600 XLM-V2-M multiparameter probe and the sediment temperature measurements with a stainless steel sediment temperature probe (Therma Plus, Electronic Temperature instruments Ltd, Worthing, West Sussex, UK, accuracy ±0.10 °C). Moreover, at the River Vantaa study site, RW temperature and EC were measured at one-hour intervals 0.3 m below the water surface and 0.3 m above the river bottom, the total depth of the water being 1.6 m. At the shallow River Palojoki study site, similar continuous measurements were performed 0.2 m above the river bottom, the total depth of the RW in the low-flow season being at most measuring points only 0.7–1.0 m.

3.2 Stable isotopes and DSi

Stable isotopic compositions of water have widely been applied as tracers in hydrological research (Gibson et al., 2005). Precipitation and GW are the main components of water in most rivers, and the relative proportions of these sources differ in each watershed, depending on the physical settings and climatic variables, as well as human activities in the watershed (Kendall and Coplen, 2001). As the basin size increases, the isotopic compositions of rivers are increasingly affected by subsequent alterations of the different runoff components and precipitation, mixing with GW, and by evaporation

HESSD
12, 2435–2476, 2015

(Kendall and Coplen, 2001). When GW and SW have different chemical signatures, spatial variation in the tracer concentration of SW can be used to verify GW inflow into the SW body (Gat and Gonfiantini, 1981; Kendall et al., 1995).

Precipitation contains little or no DSi (Asano, 2003), whereas the arithmetic mean concentration of DSi in GW for Finnish dug wells is 6.5 ppm (Lahermo et al., 2002). The DSi concentrations are dependent on the GW residence time and the grain size of aquifer media (Sandborg, 1993; Soveri et al., 2001). Streams show systematic variation in the DSi concentration as a function of flow, with higher concentrations under baseflow conditions and the lowest concentrations under high flow (Neal et al., 2005). Therefore, DSi could serve as a potential tracer to estimate the contribution of GW to river flow, as earlier observed by Hinton et al. (1994).

Water sampling of RW and GW under low-flow conditions was performed at six study sites in order to examine the impacts of GW discharge on RW chemistry at the GW discharge locations identified with AIR in 2010 (Nygård, 2011; Korkka-Niemi et al., 2011) and 2011 (Fig. 1a). Samples for δD, δ^{18}O and DSi analysis were collected from RW (n = 36) and GW (n = 26) in June, July and August 2011.

The sample locations at each study sites were selected in order to detect changes in RW chemistry: (1) upstream sample sites above potential GW discharge to the river, (2) GW discharge sites based on geological location (riverbeds overlaps glacigenic sediments) and (3) sample sites downstream of GW discharge.

The RW samples were collected from the river channel using a Limnos sampler or bottle sampler, depending the channel width and depth at the sampling location. The spring water samples were collected from discharging GW directly into sampling bottles. GW samples from observations wells were taken with a GW pump (Tempest/Twister) after purging the water volume three times. The GW samples from water intake wells were taken from the well tap after approximately 5 min of running. Samples for isotopic and DSi analysis were collected into HDPE bottles and analysed with a Picarro analyser and ICP-MS, respectively, at the Department of Geosciences and Geography, University of Helsinki. The isotope results are reported as δ values, repre-

HESSD
12, 2435–2476, 2015

senting the deviation in per mill (‰) from the isotopic composition of Vienna Standard Mean Ocean Water (VSMOW), such that $\delta^{18}O$ or $\delta D = [(R_{sample}/R_{standard}) - 1] \times 1000$, where R refers to the $^{18}O/^{16}O$ or D/H ratios in both the sample and standard. The accuracy for a single analysis was $\leq \pm 0.5$ ‰ for δD and $\leq \pm 0.1$ ‰ for $\delta^{18}O$. Samples for DSi concentration measurements were preserved in a refrigerator until analysis, pre-filtered (0.45 µm) and analysed according to the ISO 17294-2 standard. The analytical error was approximately ±2 % for DSi.

The deuterium excess (d-excess) was calculated as an index of the evaporation effect for each sample using the following equation (Dansgaard, 1964)

$$\text{d-excess} = \delta_D - 8\delta_{18}. \quad (1)$$

where δ_D is the δD and δ_{18} is the $\delta^{18}O$.

3.3 Statistics

The non-parametric Mann–Whitney U test for two unrelated or independent populations (Rock, 1988; Ranta et al., 1991) were performed using IBM SPSS Statistics 22 on RW samples ($n = 36$) in order to assess the GW component. RW sampling points were grouped according to their relationship with the aquifers. If a sampling point was inside the mapped GW area (classified aquifer), the sampling point was classified into the group "GW effect" ($n = 17$). Otherwise, the sampling point was classed as "no GW effect" ($n = 19$).

4 Results

4.1 AIR

Almost ~ 10 000 thermal images were acquired during the AIR survey in 2010 (Korkka-Niemi et al., 2012). Based on the AIR surveys and site-specific field measurements,

HESSD
12, 2435–2476, 2015

thermal anomalies were classified as discrete or multiple springs, cold creeks discharging into a river, diffuse sources by the shoreline, and diffuse and wide seepage areas (Korkka-Niemi et al., 2012).

Approximately 30 000 thermal images were acquired during the AIR survey in 2011, and the anomalies were classified into three categories. Two discrete categories (springs and cold creeks) were the same as in 2010, and a thermal anomaly was defined as a difference of at least 0.5 °C between the T_{minr} in the main channel and the observed anomaly. In this paper, the two previously presented diffuse categories were merged to form one diffuse category (wetlands), because both contribute to the diffuse discharge of GW in the riparian zone. Category three, diffuse anomalies, was located in riparian areas and had a variable areal coverage ranging from separate small diffuse anomalies to wetlands with a large areal coverage. Altogether, 374 thermal anomalies were identified along the 203 km course of the studied rivers in 2010 and 2011 using AIR (Fig. 4a and Table 2). The observed anomalies in category one were mostly connected to Quaternary deposits, whereas anomalies in categories two and three were not directly connected to them (Fig. 4).

There was significant variation in the longitudinal profiles of T_{minr} between the studied rivers (Figs. 4b and 5). The revealed patterns of spatial variability in T_{minr} provided a means to characterize the thermal signatures of the individual rivers. The most notable tributary confluences, rapids, springs, wetlands, dams and geomorphological features of the channel are marked on the profiles in Fig. 5.

The Rivers Herajoki and Vantaa showed a downstream warming trend and the headwater springs could be observed as T_{minr} lows in thermal longitudinal profiles (Fig. 5a and b). The River Vantaa showed large variability in T_{minr} of values (16 °C) over a 64 km length from the headwaters (Fig. 5a). The narrow river channel and the riparian vegetation hampered the reliable acquisition of thermal imaginary over the headwater area of the River Herajoki.

The Rivers Keravanjoki and Tuusulanjoki originate at the outflow of a lake, which could be observed as a high T_{minr} in the headwaters (Fig. 5c and d). In the River

HESSD
12, 2435–2476, 2015

Keravanjoki, a series of peaks and troughs were recorded in T_{minr} in the downstream direction, and the downstream temperatures were close the headwater temperatures (Figs. 4b and 5c). The T_{minr} varied by approximately 3 °C in the River Tuusulanjoki, and lower temperatures in the upstream part of the river were connected to a dam and small springs in the esker area (Fig. 5d).

The T_{minr} of the River Lepsämänjoki increased approximately 8 °C along the first 11 km from the headwaters, reached the maximum values at around 11 km, and after this the T_{minr} remained between 19–21 °C (Figs. 4b and 5e). In the River Lepsämänjoki, the narrowness of the channel and riparian vegetation limited thermal imagining of the headwater stream. Large springs were identified in the more distal headwater area.

The River Palojoki displayed a general downstream cooling pattern and rather constant T_{minr} values before crossing the esker aquifer area close to the artificial GW plant, where the temperatures dropped in a distinct way as the artificial and natural GW discharged into the river (Fig. 5f). The T_{minr} temperatures slowly increased after a major drop until the river entered a second esker aquifer area and temperatures started to decrease due to the influence of GW–RW exchange (Fig. 5f).

The observed smaller peaks and troughs in longitudinal temperature profiles, with 1–2 °C fluctuations in T_{minr}, were connected to the inputs from tributaries, dams, rapids, narrowing of the channel and meandering bends (Fig. 5).

The profiles were not corrected with respect to the increased RW temperatures during the flights. During mid-afternoon surveys in July, the RW temperature changed at rates of 0.2–0.7 °C h^{-1} according to the continuous water temperature monitoring in the River Vantaa. The flight times over the Rivers Palojoki, Herajoki and Tuusulanjoki were around or less than 15 min, and downstream warming therefore had only a minor effect.

The values of T_r were within ±0.6 °C of the reference measurements of T_k ($n = 29$) in subsequent years. The average absolute temperature difference between T_r and T_k was 0.22 °C. In this study, the focus was more on the relative temperature differences than the absolute temperature values.

HESSD
12, 2435–2476, 2015

4.2 Field measurements

Variable temperature anomalies in the lower RW layer, not detectable with AIR, could be characterized (Figs. 6 and 7). At the River Vantaa study site, where a series of springs was observed near the eastern shoreline prior to the major GW discharge location (Korkka-Niemi et al., 2012), the longitudinal profile (A–AA′) of RW temperatures near the sediment–water interface revealed the lower cold water regime in the river (Fig. 6a).

In general, the bottom RW temperatures were relatively equal and constant during the continuous water temperature monitoring period (Fig. 6). However, a significant difference was observed at the end of the monitoring period, when the temperature and EC values of RW at the bottom simultaneously dropped several times (Fig. 6b). The RW level declined by 0.1 m during the monitoring period due to the low precipitation in July, resulting in surges of GW from the springs near the eastern shoreline to the river bottom. The lower EC values had a statistically significant ($p < 0.01$) and very strong positive correlation (ϱPearson = 0.92, $n = 231$) with the lower temperatures on the river bottom (Fig. 6). EC values of western GW and RW were similar, respectively 22 and 21 mS m^{-1}, whereas the mean EC value of spring water on the more pristine eastern river bank was 17 mS m^{-1}. The lower EC values of RW had a statistically significant ($p < 0.01$) and strong positive correlation (ϱPearson = 0.85, $n = 145$) with the lower temperatures of RW.

The temperature of RW was 22–25 °C in the cross-sections B–BB′, C–CC′ and J–JJ (Fig. 6c). From cross-sections D–DD′ and E–EE′ (Fig. 6c), the temperature and EC values decreased more and the thermal stratification appeared more pronounced in the cross-section from F–FF′ to I–II′ (Fig. 6c and d). Further downstream, where the river bed perpendicularly cuts an unconfined glaciofluvial esker, the temperature in both sediment and RW near the sediment–water interface in the middle of river bed was 7–13 °C (cross-sections from G–GG′ to I–II′) (Fig. 6c).

HESSD
12, 2435–2476, 2015

At the study site in the River Palojoki, where river bed is significantly shallower and narrower than the River Vantaa (Table 1) and the sediments are composed of coarse-grained sand and gravel, similar temperature and EC value patterns were recorded in the RW and river bed sediment (Fig. 7). The longitudinal profile (M–MM′) of temperature and EC values of RW near the sediment–water interface showed first the decline in values and later the increase to a constant level in a downstream direction (Fig. 7a).

The EC values measured from upstream RW (0.22 mS m^{-1}) and natural GW (0.22 mS m^{-1}) were close to each other, whereas infiltration water (EC = 0.072 mS m^{-1}) used for artificial GW recharge deviated from these figures. The lower EC values, which were similar to the infiltration water, were observed concurrently with cold RW temperatures (ϱPearson = 0.86, $p < 0.01$, $n = 133$). The lower RW temperatures occurred simultaneously with the lower EC values near the bottom during the continuous water temperature-monitoring period (Fig. 7b), and had a statistically significant ($p < 0.01$) and strong positive correlation (ϱPearson = 0.78, $n = 261$).

In the upstream cross-sections, the RW temperature was 7.2 °C at the lowest near the sediment–water interface and the low temperatures were observed in the river bed where the water depth was at the maximum (V–VV, W–WW′), whereas the RW temperature at most measurement points was 5–6 °C in cross-sections from Q–QQ′ to T–TT′ (Fig. 7c). Further downstream, the water depth in the river was 0.4–0.8 m with a temperature range from 6 to 18 °C near the sediment–water interface in cross sections from N–NN′ to P–PP′ (Fig. 7c). The water temperature throughout the entire river bed at the River Palojoki study site was generally lower than in the River Vantaa study site (Figs. 6 and 7).

4.3 Stable isotopes and DSi

The measured mean δ^{18}O, δD, DSi and d-excess values of water samples are presented in Tables 3 and 4. There were significant differences in stable isotope composition between the studied rivers (Table 3). The ranked order of the mean δ^{18}O and δD values of rivers from the most enriched to the least enriched were River Keravan-

HESSD
12, 2435–2476, 2015

joki, River Tuusulanjoki, River Palojoki, River Vantaa, River Lepsämänjoki and River Herajoki (Table 3).

Significant variation in DSi concentrations was observed between the studied rivers (Table 4). Comparing the six rivers, the mean DSi concentrations were highest in the Rivers Lepsämänjoki and Herajoki (Table 4). The ranked order of the mean DSi concentrations of rivers from the lowest to the highest were River Keravanjoki, River Tuusulanjoki, River Vantaa, River Palojoki, River Lepsämänjoki and River Herajoki (Table 4).

5 Discussion

5.1 AIR

There were some variations in the observed anomalies between consecutive years, possibly related to annual differences in the hydraulic head. Some minor springs identified in the AIR survey in July 2010 were not detectable in July 2011, because the hydraulic heads of the aquifers in study area were generally at a higher level in July 2010 than in July 2011. This illustrates the temporal as well as the spatial variation in GW–RW interaction in the studied rivers. The differences observed between years are partially related to the different method of image acquisition (hand-held vs. mounted) and missing some short sections of the strongly meandering study rivers.

The differences in thermal anomalies among the studied streams can partly be explained by the shape of the river beds and composition of the river bed sediments. For instance, most parts of the River Herajoki have a fine-grained stream bed, and because no preferential flow paths are available for GW, the number of observed anomalies was lower. Conversely, in the River Palojoki, several sections have an influx of GW through the bottom and shoreline slopes of the coarse-grained gravelly and sandy stream bed.

The lower temperatures in the rapid zones were generally due to the increase in the stream velocity, mixing of the water layers and disappearance of stratification. Moreover, the rapids appear in areas of coarse-grained sediments and possibly enhanced

HESSD
12, 2435–2476, 2015

GW discharging into the river. The meander bends and narrowing of the stream channel had a similar effect on the mixing of the RW. According to Torgersen et al. (2001), large-scale patterns such as gradual warming trends covering 5–10 km are related physical geomorphic and hydrological processes at the watershed scale. These types of patterns were seen, for example, in the River Keravanjoki, where gradual decreasing and increasing trends were connected to the wetland and notable widening of the main channel, respectively (Fig. 5c).

The longitudinal thermal profiles of the Rivers Keravanjoki and Vantaa in consecutive summers revealed similar overall thermal patterns and amplitudes, although the absolute temperatures differed, being lower in 2011 (Fig. 5a and c). In 2010, July was exceptionally warm and the SW temperatures were close to the record level (Korhonen and Haavalammi, 2012), which possibly explains the observed higher T_{minr}. Correspondingly, the differences in headwater conditions, precipitation, and main channel and tributary flow rates influenced the magnitude of the longitudinal thermal profile as described by Cristea and Burges (2009). The longitudinal thermal patterns indicated that the cool and warm water sources mainly had spatially fixed locations (Fig. 5a and c), as also earlier demonstrated by Faux et al. (2001). Longitudinal thermal patterns are a result of the interaction of natural environmental and anthropogenic factors (Faux et al., 2001). The stream temperature is an important parameter in aquatic management (Poole and Berman, 2001), and thermal profiles can provide valuable insights into the causative factors behind the observed stream temperatures.

5.2 Field measurements

The GW discharge locations identified using AIR were confirmed with RW and sediment temperature measurements in 2010, as reported in Nygård (2011). EC values have in earlier studies on groundwater–lake water interactions proved to be a good indicator of the GW influence on surface waters, the average EC value in GW normally being significantly higher than in lake water (Korkka-Niemi et al., 2009; Korkka-Niemi et al., 2011). However, in the river systems EC values range widely both temporally and

HESSD
12, 2435–2476, 2015

spatially. Hence the use of EC as an indicator of the GW influence is not as straightforward as in GW-lake water studies.

The GW discharging into the River Vantaa appeared as lower temperature and EC values in cross-sections from D–DD′ to I–II′ (Fig. 6c). The sediment temperatures were also low (6–12 °C) along the river banks due to the continuous discharge of GW through the sandy shoreline deposits. The river flow rate measurements by Brander (2013) with a RiverSurveyor® M9 Acoustic Doppler Current Profiler (SonTek) demonstrated that in the low-flow period, the river flow within this major GW discharge location increased by approximately 0.1 $m^3 s^{-1}$, i.e. 8640 $m^3 d^{-1}$. The cross-sections B–BB′, C–CC′ and J–JJ represent conditions before and after GW discharge into the river (Fig. 6c).

At the River Palojoki study site, the AIR survey revealed a lowering of several degrees in surface temperatures of RW downstream from the esker formation (Fig. 5f), indicating that a significant proportion of the water in the River Palojoki originates from the semi-confined glaciofluvial aquifer. The river flow measurements reported by Brander (2013) also indicated an increase of 0.044 $m^3 s^{-1}$ (3800 $m^3 d^{-1}$) in river flow from a water intake plant to a location downstream. The fluctuations of RW temperature and EC values during the continuous water temperature-monitoring period (Fig. 7) can be an outcome of the river level fluctuations and pumping from the production wells, resulting in surges of artificial GW. The observed differences in thermal surveys between the Rivers Vantaa and Palojoki are related to the geomorphological properties and flow conditions of the river channels.

The invisibility of GW discharge in thermal images of the River Vantaa study site is related to the thermal stratification of RW. The highest volumes of GW were observed to discharge to the river at the point where the river bed perpendicularly cuts the esker ridge. At this point, the temperature differences between the surface and bottom RW temperatures were as great as 17 °C. Thermal stratification is an outcome of both the influx of cold water and retention of cold and dense water at the bottom of the river channel pools, as reported by Nielsen et al. (1994). The cold and dense water originates from both GW sinking down by the river bank and possibly through subsurface

HESSD
12, 2435–2476, 2015

preferential GW flow paths into the lower part of the river channel (Fig. 6d). This cold and less turbulent lower water regime can be isolated from mixing with the warm and more turbulent upper water regime as long as the inflow of cold water is sufficient or the river flow rate is slow enough, according to Nielsen et al. (1994). Matthews et al. (1994) suggested that thermal stratification is possible if cold water enters the river at locations with a very low flow rate.

Considerable thermal stratification was also observed at the Palojoki study site, as the maximum difference between surface and bottom RW was 13.4 °C. The thermal stratification was strongest at the pool and disappeared (with decreasing water depth) in a downstream direction (Fig. 7c). As Torgersen at al. (2001) pointed out, thermal remote sensing can be biased by thermal stratification in channels with subsurface cold water inputs during low river flow rates. In the AIR survey results, the potential existence of these "hidden" GW–RW interaction sites should especially be noted during periods with low river flow rates.

5.3 Stable isotopes and DSi

The isotopic composition of shallow GW does not differ significantly from the mean weighted annual composition of precipitation in temperate climates (Clark and Fritz, 1997). According to Kortelainen and Karhu (2004), the isotope composition of shallow GW follows the local meteoric water line (LMWL) in Finland. The measured mean $\delta^{18}O$ and δD of springs, GW and well water are mainly in close agreement with the previous studies of Kortelainen and Karhu (2004) (Table 3). However, the $\delta^{18}O$ and δD values of the observation well close to the Tuusula water intake plant were slightly displaced to the right of the LMWL, which was related to evaporation effects (Fig. 8a). These more evaporated $\delta^{18}O$ and δD values from the observation well can be related RW recharging the aquifer. Brander (2013) demonstrated with river flow rate measurements that the river flow decreased by approximately 8 % (0.07 $m^3 s^{-1}$, i.e. 6300 $m^3 d^{-1}$) due to RW recharging the aquifer in the low-flow period.

HESSD
12, 2435–2476, 2015

The stable isotope composition of the majority of the world's main rivers falls along the global meteoric water line (GMWL) (Rozanski et al., 2001). The GMWL has a d-excess value of 10 ‰ (Merlivat and Jouzel, 1979), and d-excess values significantly below the global average of 10 ‰ indicate evaporation, since falling as precipitation (Kendall and Coplen, 2001). Among the studied rivers, the River Herajoki had d-excess values indicating the smallest evaporation effects. The Rivers Vantaa and Lepsämänjoki were slightly dislocated from the LMWL and the d-excess values indicated some evaporation effects (Fig. 8b).

The stable isotope composition of River Herajoki plotted along the LMWL, with a stable isotope composition close to the GW composition, indicating GW as a source component (Fig. 8b). Brander (2013) observed from river flow measurements that the RW recharged the underlying aquifer in the proximity of a water intake plant. However, in this study, RW infiltration into the wells could not been observed due to the similarity of δ^{18}O and δD values in GW and RW.

The δ^{18}O and δD values of Rivers Keravanjoki and Tuusulanjoki were significantly displaced to the right of the LMWL, which was related to evaporation effects in open water bodies (Table 3, Fig. 8b). The RW sample taken from River Tuusulanjoki (esker aquifer area) in August 2011 deviated from other RW samples in having a stable isotope composition close to that of the GW (Fig. 8b). The more evaporated δ^{18}O, δD and d-excess values of Rivers Keravanjoki and Tuusulanjoki could be due to the existence of headwater lakes and the dams along the river path. Additionally, supplementary water (Lake Päijänne water) is released into River Keravanjoki via the headwater Lake Ridasjärvi to sustain a sufficient river flow and water quality in river channel during the summer months (Vahtera et al., 2012) (Fig. 1a). Altogether, 3.9 10^6 m^3 of Lake Päijänne water was released, with an average discharge of 0.50 m^3 s^{-1} from 25 May 2011 to 22 August 2011 (Vahtera et al., 2012). Supplementary water (Lake Päijänne water) was also released into the upstream lake of the River Tuusulanjoki to improve the water quality. Lake Päijänne water has significantly evaporated δ^{18}O, δD and d-excess values of −8.96, −71.5 and −0.1 ‰, respectively, and a low DSi concentration (1.2 ppm).

HESSD
12, 2435–2476, 2015

This can have a considerable effect on the $\delta^{18}O$, δD, d-excess and DSi values of the River Keravanjoki and some effect on the respective values of the River Tuusulanjoki. The $\delta^{18}O$ and δD values of the River Palojoki were a spatiotemporally varying complex mixture of precipitation, run off, and natural and artificial GW. More detailed sampling is needed in order to specify the different contributions to the river flow.

The measured mean DSi values of springs, GW and well water were slightly higher than in Finnish dug wells in general (Lahermo et al., 2002) (Table 3). In Rivers Lepsämänjoki and Herajoki, the observed DSi concentrations were somewhat higher than in Finnish streams generally (Lahermo et al., 1996; range from 0.80 to 6.86 ppm, mean 3.62 ppm, $n = 1162$), suggesting a greater GW component than typically. The mean DSi concentrations of the Rivers Vantaa and Palojoki were close to the DSi in Finnish streams generally. The low DSi concentrations of the Rivers Keravanjoki and Tuusulanjoki can be related to the supplementary addition of Lake Päijänne water.

The DSi concentrations of RW are an outcome of the relative proportions of different water types (GW, soil water, runoff, direct channel precipitation), the residence times of water in the soil matrix, land use, geology, weathering intensity, climatic variation and diatom production (Scanlon et al., 2001; Conley, 1997). Consequently, these multifarious and overlapping factors can complicate the use of DSi as a GW tracer in the riverine environment. However, in this study, the results for stable isotope compositions were mainly consistent with the DSi concentrations, as higher DSi concentrations appeared coincident with the stable isotope composition typical to the GW. The usability of DSi as a GW tracer was limited by the variability in the GW end member concentrations, and use of the DSi as a GW tracer would benefit from the spatiotemporally denser sampling of GW end members.

Mean $\delta^{18}O$, δD, d-excess and DSi values for RW impacted by aquifers were −10.05, −75.5, 4.9 ‰ and 4.6 ppm, respectively, while the respective values for RW not so clearly related to aquifers were −9.49, −73.1, 2.9 ‰ and 2.9 ppm. According to the non-parametric Man-Whitney U test, there was a statistically significant difference ($p < 0.05$) between the "GW effect" sites and "no GW effect" sites in the measured

HESSD
12, 2435–2476, 2015

DSi and d-excess values. This indicates that the GW input could also be seen in RW quality at the observed interaction sites. Therefore, these interaction sites could be more important for water quality and quantity than has thus far been acknowledged. GW discharge can have a positive effect on a river by increasing the river flow and improving water quality in the low-flow season. Alternatively, river channels hydraulically connected to aquifers can have a negative effect on water intake plants in the high-flow season. Nutrients (nitrate and phosphate) and faecal contamination (human sewage or animal sources) are the main causes of lowered water quality of the River Vantaa and its tributaries. These sources induce risks to GW in the high-flow season. In the studied river sections, there are 12 municipal water intake plants in close proximity to the river channel and located close to the GW–RW interaction sites identified in this study (Fig. 4a). These water intake plants can pose a potential risk of water quality deterioration due to RW infiltration into the aquifer during floods. The identification and localization of GW–RW interaction sites (as potential risks sites) would enable water management activities (e.g. reducing the water volume pumped from production wells nearest the river channel in the most critical period when the RW level is high) to prevent a deterioration in GW quality at pumping wells.

6 Conclusions

In the River Vantaa and its tributaries, around 370 GW–RW interaction sites could be located with AIR along the studied rivers. GW–RW exchange was notable and influenced the main stream temperatures in some river sections. AIR revealed some temporal variation in GW–RW interaction in the Rivers Keravanjoki and Vantaa. However, the main GW–RW interaction sites could be observed in both study years. The longitudinal T_{minr} profiles displayed considerable spatial variability both within and among the rivers. These variations are outcomes of processes occurring at both the watershed and local scales.

HESSD
12, 2435–2476, 2015

AIR was found to be an applicable method to identify thermal anomalies and possible areas of GW discharge across the river basin and to collect spatially continuous patterns of RW temperatures in entire river sections over a short period of time. Furthermore, AIR can also direct water sampling and further investigations to the relevant GW–RW interaction locations.

The GW discharge locations identified with AIR were confirmed with RW and sediment temperature measurements. GW input through the river bottom was detected from field measurements as lower temperature anomalies near the sediment–water interface. Thermal stratification can bias the AIR results, leading to an underestimation of the extent and magnitude of the GW–RW interaction, as only surficial temperature anomalies can be detected, and should be taken account in AIR surveys during low-flow conditions in the summer. The results of this study support the use of several methods simultaneously to survey and confirm the GW–RW interaction.

In addition to temperature, stable isotopic compositions, EC and DSi concentrations of RW can be applied as tracers in the River Vantaa and its tributaries in order to verify the observed GW discharge into the river system or RW recharge into the aquifer. The stable isotopes and DSi revealed that in smaller tributaries, the water flowing in the streams is predominantly GW originating from the headwater aquifers in the low-flow period. This was also supported by the cold RW temperature in headwater areas observed with AIR.

The interaction locations identified during the low-flow season in July 2010 and 2011 should be considered as potential risk areas for the 12 water intake plants during floods, and should be taken under consideration in RW basin management under changing climatic situations. Climate change is predicted to result in increasing floods, which could increase the vulnerability to contamination of water intake plants located in proximity to main stream channels due to the RW. During base flow, the narrow and shallow streams in the catchment are predominantly composed of GW originating from the adjacent aquifers. Conversely, during the maximum river flow periods, the RW can recharge the adjacent aquifer, and risk management activities targeted at controlling

HESSD
12, 2435–2476, 2015

bank infiltration are needed at several sites utilized by water works. Moreover, to quantify the volumes of GW discharge into the river beds as well as the bank infiltration from streams to the aquifers during peak-flow periods, river flow rate measurements recommended. This research provided new insights for water management, and the results could be used in evaluating the possible effects of GW and RW exchange on water quality in the identified exchange zones.

Acknowledgements. Petri Pellikka, Tuuli Toivonen and Pasi Valkama assisted in the fieldwork during the summers of 2010 and/or 2011. The research was funded by the Maa- ja Vesitekniikan Tuki Foundation, the K.H. Renlund Foundation, Hyvinkää Water, Nurmijärvi Water, Riihimäki Water, the Water Supply Company of the Tuusula Region, Uusimaa Centre for Economic Development, Transport and the Environment, the Water Protection Association of the River Vantaa and Helsinki Region and the Department of Geosciences and Geography, University of Helsinki.

References

Asano, Y., Uchida, T., and Ohte, N.: Hydrologic and geochemical influences on the dissolved silica concentration in natural water in a steep headwater catchment, Geochim. Cosmochim. Ac., 67, 1973–1989, doi:10.1016/S0016-7037(02)01342-X, 2003.

Beniston, M., Stephenson, D. B., Christensen, O. B., Ferro, C. A. T., Frei, C., Goyette, S., Halsnaes, K., Holt, T., Jylhä, K., Koffi, B., Palutikof, J., Schöll, R., Semmler, T., and Woth, K.: Future extreme events in European climate: an exploration of regional climate model projections, Climatic Change, 81, 71–95, 2007.

Boulton, A. J., Findlay, S., Marmonier, P., Stanley, E. H., and Valett, H. M.: The functional significance of the hyporheic zone in streams and rivers, Annu. Rev. Ecol. Syst., 29, 59–81, 1998.

Brander, M.: Virtaamamittaukset tutkimusmenetelmänä pohjaveden purkautumismäärien sekä jokiveden ja pohjaveden sekoittumissuhteiden arvioinnissa Vantaanjoen valuma-alueen jokiuomissa, MSc thesis, University of Helsinki, Finland, 2013.

HESSD

12, 2435–2476, 2015

Breilin, O., Paalijärvi, M., and Valjus, T.: Pohjavesialueen geologisen rakenteen selvitys I Salpausselällä Hyvinkään kaupungissa Nummenkärki-Suomiehensuo alueella, Arch. Rep.17/2014, Geol. Surv. of Finland, Espoo, 89 pp., 2004 (in Finnish).

Brunke, M. and Gonser, T.: The ecological significance of exchange processes between rivers and groundwater, Freshwater Biol., 37, 1–33, 1997.

Clark, I. D. and Fritz, P.: Environmental Isotopes in Hydrogeology, Lewis Publishers, Boca Raton, FL, 328 pp., 1997.

Conant, B. and Mochnacz, N. J.: Low-altitude and land-based infrared thermography to identify types of groundwater discharge in NWT streams, in: 2009 Joint Assembly, American Geophysical Union, Toronto, Ontario, 24–27 May, H72A-02, 2009.

Conley, D. J.: Riverine contribution of biogenic silica to the oceanic silica budget, Limnol. Oceanogr., 42, 774–777, 1997.

Cristea, N. C. and Burges, S. J.: Use of thermal infrared imagery to complement monitoring and modeling of spatial stream temperature, J. Hydraul. Eng.-ASCE, 14, 1080–1090, 2009.

Dansgaard, W.: Stable isotopes in precipitation, Tellus, 16, 436–468, 1964.

Davis, J. B.: Aerial thermography surveys to detect groundwater discharge in the St. Johns river water management district, Northeast Florida, in: ASPRS 2007 Annual Conference Tampa, Florida, 7–11 May, 174–182, 2007.

Ekholm, M.: Suomen vesistöalueet, Publ. Serie A 126, National Board of Waters and the Environment, Helsinki, 166 pp., 1993.

Faux, R. N., Lachowski, H., Maus, P., Torgersen, C. E., and Boyd, M. S.: New Approaches for Monitoring Stream Temperature: Airborne Thermal Infrared Remote Sensing, Project Rep., Remote Sensing Applications Laboratory, USDA Forest Service, Salt Lake City, UT, 32 pp., 2001.

Gat, J. R. and Gonfiantini, R.: Stable Isotope Hydrology: Deuterium and Oxygen-18 in the Water Cycle, IAEA Tech. Rep. Series No. 210, IAEA, Vienna, 339 pp., 1981.

Gibson, J. J., Edwards, T. W., Birks, S. J., St Amour, N. A., Buhay, W. M., McEachern, P., Wolfe, B. B., and Peters, D. L.: Progress in isotope tracer hydrology in Canada, Hydrol. Process., 19, 303–327, 2005.

Hansen, E. A.: Some effects of groundwater on brown trout, T. Am. Fish. Soc., 104, 100–110, 1975.

HESSD
12, 2435–2476, 2015

Hatva, T.: Iron and Manganese in Groundwater in Finland: Occurrence in Glaciofluvial Aquifers and Removal by Biofiltration, Publ. of the Water and Environmental Istitute 4, National Board of Waters and the Environment, Helsinki, 1989.
Helmisaari, H.-S., Illmer, K., Hatva, T., Lindroos, A.-J., Miettinen, I., Pääkkönen, J., and Reijonen, R.: Tekopohjaveden muodostaminen: imeytystekniikka, maaperäprosessit ja veden laatu, TEMU Final Rep., Research Papers 902, METLA, Vantaa, 2003 (in Finnish).
Helsinki-Uusimaa Region: Vantaanjoen kehittämisohjelma, Publ. B18, Helsinki, 1997 (in Finnish).
Hinton, M. J., Schiff, S. L., and English, M. C.: Examining the contributions of glacial till water to storm runoff using two- and three-component hydrograph separations, Water Resour. Res., 30, 983–993, 1994.
Jylhä, K., Tuomenvirta, H., and Ruosteenoja, K.: Climate change projections for Finland during the 21st century, Boreal Environ. Res., 9, 127–152, 2004.
Karlsson, K.-P.: Atlas of Finland, Folio 132, Water, National Board of Survey and Geographical Society of Finland, Helsinki, 31 pp., 1986.
Kendall, C. and Coplen, T. B.: Distribution of oxygen-18 and deuterium in river waters across the United States, Hydrol. Process., 15, 1363–1393, 2001.
Kendall, C., Sklash, M. G., and Bullen, T. D.: Isotope tracers of water and solute sources in catchments, in: Solute Modelling in Catchment Systems, John Wiley and Sons, New York, 261–303, 1995.
Korhonen, J. and Haavanlammi, E.: Hydrological Yearbook 2006–2010, The Finnish Environment 8/2012, Finnish Environmental Institute, Helsinki, 2012.
Korkka-Niemi, K., Rautio. A., and Wiebe, A.: Methods for investigating groundwater surface water interaction at Lake Pyhäjärvi, SW Finland, in: 6th National Geological Colloquium program and abstracts, Publications of the Department of Geology Series A 3, Helsinki, Finland, 4–6 March 2009, 2, 2009.
Korkka-Niemi, K., Rautio, A., Niemistö, P., and Karhu, J.: Hydrogeochemical and isotopic indications of ground water–surface water interaction at Lake Pyhäjärvi, SW Finland, in: GQ2010: Groundwater Quality Management in a Rapidly Changing World, edited by: Schirmer, M., Hoehn, E., and Vogt, T., IAHS Publ., 342, 423–426, 2011.
Korkka-Niemi, K., Kivimäki, A.-L., Lahti, K., Nygård, M., Rautio, A., Salonen, V.-P., and Pellikka, P.: Observations on groundwater-surface water interaction, River Vantaa, Finland, Management of Env. Quality, 23, 222–231, 2012.

HESSD
12, 2435–2476, 2015

Kortelainen, N.: Isotopic Fingerprints in Surficial Waters: Stable Isotope Methods Applied in Hydrogeological Studies, Geol. Surv. of Finland 41, Espoo, 55 pp., available at: http://arkisto.gtk.fi/ej/ej66synopsis.pdf (last access: December 2014), 2007.

Kortelainen, N. M. and Karhu, J. A.: Regional and seasonal trends in the oxygen and hydrogen isotope ratios of Finnish groundwaters: a key for mean annual precipitation, J. Hydrol., 285, 143–157, 2004.

Kortelainen, N. M. and Karhu, J. A.: Tracing the decomposition of dissolved organic carbon in artificial groundwater recharge using carbon isotope ratios, Appl. Geochem., 21, 547–562, 2006.

Kuusisto, E.: Suomen tulvat ovat jo muuttuneet (Floods in Finland Have Already Changed), Vesitalous, Helsinki, 1, 126–128, 2015.

Lahermo, P., Väänänen, P., Tarvainen, T., and Salminen, R.: Geochemical Atlas of Finland, Part 3: Environmental Geochemistry – Stream Waters and Sediments, Geol. Surv. of Finland, Espoo, Finland, 1996.

Lahermo, P., Tarvainen, T., Hatakka, T., Backman, B., Juntunen, R., Kortelainen, N., Lakomaa, T., Nikkarinen, M., Vesterbacka, P., Väisänen, U., and Suomela, P.: Tuhat kaivoa – Suomen kaivovesien fysikaalis – kemiallinen laatu vuonna 1999 (One Thousand Wells – the Physical-Chemical Quality of Finnish Well Waters in 1999), Rep. of Investigation 155, Geol. Surv. of Finland, Espoo, 2002 (in Finnish with English abstract).

Loheide, S. P. and Deitchman, R. S.: A Thermal Remote Sensing Tool for Mapping Spring and Diffuse Groundwater Discharge to Streams, Final Rep. WR07R005, Water Resources Institute, University of Wisconsin, 2009.

Loheide, S. P. and Gorelick, S. M.: Quantifying stream–aquifer interactions through the analysis of remotely sensed thermographic profiles and in situ temperature histories, Environ. Sci. Technol., 40, 3336–3341, 2006.

Matthews, K. R., Berg, N. H., Azuma, D. L., and Lambert, T. R.: Cool water formation and trout habitat use in a deep pool in the Sierra Nevada, California, T. Am. Fish. Soc., 123, 549–564, 1994.

Merlivat, L. and Jouzel, J.: Global climatic interpretation of the deuterium-oxygen 18 relationship for precipitation, J. Geophys. Res., 84, 5029–5033, 1979.

Mäntylä, K. and Saarelainen, S.: Rakennetun ympäristön sopeutuminen ilmastonmuutoksen aiheuttamille tulvavaikutuksille, Tutkimuskohteena Vantaanjoki, Res. Rep. VVT-R-04429-08, VTT Technical Research Centre of Finland, 180 pp., 2008 (in Finnish).

HESSD
12, 2435–2476, 2015

Neal, C., Neal, M., Reynolds, B., Maberly, S. C., May, L., Ferrier, R. C. Smith, J., and Parker, J. E.: Silicon concentrations in UK surface waters, J. Hydrol., 304, 75–93, 2005.
Nielsen, J. L., Lisle, T. E., and Ozaki, V.: Thermally stratified pools and their use by steelhead in northern California streams, T. Am. Fish. Soc., 123, 613–626, 1994.
Nygård, M.: Jokien hydrauliset yhteydet pohjavesimuodostumiin Vantaanjoen valuma-alueella lämpötila – ja vedenlaatuaineistojen perusteella, M.Sc. thesis, University of Helsinki, Finland, 2011.
Pirinen, P., Simola, H., Aalto, J., Kaukoranta,. J.-P., Karlsson, P., and Ruuhela, R.: Climatological Statistics of Finland 1981–2010, Rep. No. 2012, Finnish Meteorological Institute, Helsinki, 1, 2012.
Poole, G. C. and Berman. C. H.: An ecological perspective on in-stream temperature: natural heat dynamics and mechanisms of human-caused thermal degradation, Environ. Manage., 27, 787–802, 2001.
Ranta, E., Rita, H., and Kouki, J.: Biometria, tilastotiedettä ekologeille, Yliopistopaino, Helsinki, 569 pp., 1991 (in Finnish).
Rock, N. M. S.: Numerical Geology: a Source Guide, Glossary and Selective Bibliography to Geological Uses of Computers and Statistics Numerical Geology, Lecture Notes in Earth Sciences, Vol. 18, Springer-Verlag, Berlin, 427 pp., 1988.
Rosenberry, D. O. and LaBaugh, J. W.: Field techniques for estimating water fluxes between surface water and ground water, US Geol. Surv., Techniques and Methods 4-D2, Reston, Virginia, US Geol. Surv., 128 pp., 2008.
Rozanski, K., Froehlich, K., and Mook, W. G.: Surface water, in: Environmental Isotopes in the Hydrological Cycle: Principles and Applications, Vol. III, edited by: Mook, W. G., IHP-V, Technical Documents in Hydrology No. 39, UNESCO, Paris, 2001.
Sandborg, M.: Soranoton vaikutus pohjaveteen. Tutkimusraportti I: Pohjaveden laatuun vaikuttavien aineiden geokemiallisia ominaisuuksia (Effect of Gravel Extraction on Groundwater, Report 1: Geochemical Properties of Substances Affecting Groundwater Quality), Serie 328, National Board of Waters and the Environment, Helsinki, 1993 (in Finnish).
Scanlon, T., Scanlon, T. M., Raffensperger, J. P., and Hornberger, G. M.: Modeling transport of dissolved silica in a forested headwater catchment: implications for defining the hydrochemical response of observed flowpathways, Water Resour. Res., 37, 1071–1082, 2001.
Schneider, R. L., Negley, T. L., and Wafer, C.: Factors influencing groundwater seepage in a large, mesotrophic lake in New York, J. Hydrol., 310, 1–16, 2005.

HESSD
12, 2435–2476, 2015

Sebestyen, S. D. and Schneider, R. L.: Dynamic temporal patterns of nearshore seepage flux in a headwater Adirondack lake, J. Hydrol., 247, 137–150, 2001.
Seuna, P.: Suomen vesistöalueet: Ehdotus vesistöalueiden yleisjaoksi ja vesistötunnukseksi, Report 10, National Board of Waters, Helsinki, 1971.
Silander, J., Vehviläinen, B., Niemi, J., Arosilta, A., Dubrovin, T., Jormola, J., Keskisarja, V., Keto, A., Lepistö, A., Mäkinen, R., Ollila, M., Pajula, H., Pitkänen, H., Sammalkorpi, I., Suomalainen, M., and Veijalainen, N.: Climate change adaptation for hydrology and water resources, FINADAPT WorkingPaper 6, Finnish Environment Institute Mimeographs 335, Finnish Environment Institute, Helsinki, 2006.
Soveri, J., Mäkinen, R., and Peltonen, K.: Pohjaveden korkeuden ja laadun vaihtelusta Suomessa 1975–1999 (Changes in Groundwater Levels and Quality in Finland in 1975–1999), The Finnish Environment 420, Finnish Environmental Institute, Helsinki, 350 pp., 2001 (English summary).
Stanford, J. A. and Ward, J. V.: An ecosystem perspective of alluvial rivers: connectivity and the hyporheic corridor, J. N. Am. Benthol. Soc., 12, 48–60, 1993.
Suhonen, V. and Rantakokko, K.: Vantaanjoen tulvatorjunnan toimintasuunnitelma, Rep.1/2006, Centre for Economic Development, Transport and the Environment for Uusimaa, Helsinki, 2006 (in Finnish).
Tikkanen, M.: Geomorphology of the Vantaanjoki drainage basin southern Finland, Fennia, 167, 19–72, 1989.
Torgersen, C. E., Faux, R. N., McIntosh, B. A., Poage, N. J., and Norton, D. J.: Airborne thermal remote sensing for water temperature assessment in rivers and streams, Remote Sens. Environ., 76, 386–398, 2001.
Tóth, J.: A theoretical analysis of groundwater flow in small drainage basins, J. Geophys. Res., 68, 4795–4812, 1963.
Vahtera, H., Männynsalo J., and Lahti, K.: Vantaanjoen yhteistarkkailu – Vedenlaatu vuonna 2011, Publ. of 67/2012, The Water Protection Association of the River Vantaa and Helsinki Region, Helsinki, 94 pp., 2012.
Vahtera, H., Männynsalo, J., and Lahti. K.: Vantaanjoen yhteistarkkailu – Vedenlaatu vuosina 2011–2013, Publ. of 72/2014, The Water Protection Association of the River Vantaa and Helsinki Region, Helsinki, 93 pp., 2014.
Veijalainen, N., Sippel, K., and Vehviläinen, B.: Tulvien muuttuminen Vantaanjoella ja Espoonjoella, in: Climate is Changing in the Helsinki Metropolitan Area, Background Studies for

HESSD
12, 2435–2476, 2015

the Adaptation Strategy, Publ. 3/2010, Helsinki Region Environmental Services Authority, Helsinki, 37–53, 2009 (abstract in English).

Veijalainen, N., Lotsari, E., Alho, P., Vehviläinen, B., and Käyhkö, J.: National scale assessment of climate change impacts on flooding in Finland, J. Hydrol., 391, 333–50, 2010.

Winter, T. C., Harvey, J. W, Franke, O. L., and Alley, W. M.: Ground Water and Surface Water A Single Resource, US Geol. Surv. circular 1139, Denver, Colorado, US Geol. Surv., 87 pp., 1998.

Woessner, W. W.: Changing views of stream-ground-water interaction, in: Proceedings of American Institute of Hydrology/International Association of Hydrologists XXVIII Congress: Gambling with Groundwater, Physical, Chemical and Biological Aspects of Aquifer-Stream Relationships, St. Paul, MN, September 1998, 1–6, 1998.

Woessner, W. W.: Stream and fluvial plain ground water interactions: rescaling hydrogeologic thought, Ground Water, 38, 423–429, 2000.

HESSD

12, 2435–2476, 2015

Table 1. Field measurement study sites and their characteristics. Data on river flow rates, mean flow discharge (NQ) and mean high discharge (HQ) based on 2002–2012 data from the HERTTA database, except for the Rivers Palojoki and Herajoki, which are based on flow measurements in 2011–2012*.

River	Aquifer Type	River bed width (m)	River bed depth (m)	NQ-HQ $m^3 s^{-1}$
Vantaa	Glaciofluvial esker, unconfined	14–17	1.5–2.5	0.64–51.00
Keravanjoki	Littoral sand, semi-confined	15–25	1–2.7	0.07–48.00
Tuusulanjoki	Glaciofluvial esker + delta, unconfined	4–8	0.2–0.7	0.02–7.83
Palojoki	Glaciofluvial esker, semi-confined	3–9	0.1–1.1	0.02–2.44*
Lepsämänjoki	Glaciofluvial esker, confined	3–5	0.5–1.4	0.08–19.8
Herajoki	Glaciofluvial esker, confined	2–3	0.3–0.5	0.02–0.95*

HESSD
12, 2435–2476, 2015

Table 2. Discrete and diffuse groundwater discharge areas identified in the AIR surveys conducted in 2010 and 2011 classified into three categories.

River	Category 1 Spring/ Discrete	Category 2 Creek/ Discrete	Category 3 Diffuse	Total
Herajoki	1	1	2	4
Lepsämänjoki	25	11	19	55
Keravanjoki	40	32	53	125
Palojoki	17	6	21	44
Tuusulanjoki	6	4	14	24
Vantaa	41	23	58	122
Total	130	77	167	374

HESSD
12, 2435–2476, 2015

Table 3. The mean, range and SD of $\delta^{18}O$, δD and d-excess values of water samples in summer 2011.

Water type		$\delta^{18}O$ ‰, VSMOW			δD ‰, VSMOW			d-excess		
	n[a]	Mean[b]	Range	SD[c]	Mean[b]	Range	SD[c]	Mean[b]	Range	SD[c]
Spring	6	−11.70	0.70	0.23	−83.8	2.8	0.95	9.8	3.3	1.06
GW	6	−11.57	1.49	0.63	−83.1	9.2	3.84	9.3	3.6	1.29
Well	14	−12.10	0.55	0.14	−86.9	2.8	0.80	9.9	1.9	0.53
R. Herajoki	4	−11.18	1.33	0.54	−80.8	10.2	3.89	8.6	1.6	0.66
R. Lepsämänjoki	7	−10.08	0.85	0.28	−75.5	4.0	1.32	5.2	3.0	1.05
R. Vantaa	6	−10.12	0.98	0.38	−75.6	7.7	3.35	5.4	1.8	0.62
R. Palojoki	6	−9.63	2.52	0.96	−71.1	22.2	8.87	5.9	3.4	1.28
R. Tuusulanjoki	6	−9.70	3.19	1.06	−75.9	13.7	4.62	1.7	11.8	3.90
R. Keravanjoki	8	−8.84	2.59	1.15	−70.9	14.4	6.59	−0.2	6.4	2.65

[a] Number of analyses,
[b] Arithmetic mean,
[c] SD (1σ).

HESSD
12, 2435–2476, 2015

Table 4. The mean, range and SD of DSi values of water samples in summer 2011.

Water type	DSi, ppm			
	n[a]	Mean[b]	Range	SD[c]
Spring	6	9.8	3.3	1.14
GW	6	8.9	4.3	1.38
Well	14	8.9	4.9	1.52
R. Herajoki	4	6.9	2.8	1.14
R. Lepsämänjoki	7	6.2	2.1	0.72
R. Vantaa	6	3	2.3	1.00
R. Palojoki	6	3.4	0.5	0.16
R. Tuusulanjoki	6	2.1	6.6	2.32
R. Keravanjoki	8	2.1	0.7	0.23

[a] Number of analyses,
[b] Arithmetic mean,
[c] SD (1σ).

HESSD
12, 2435–2476, 2015

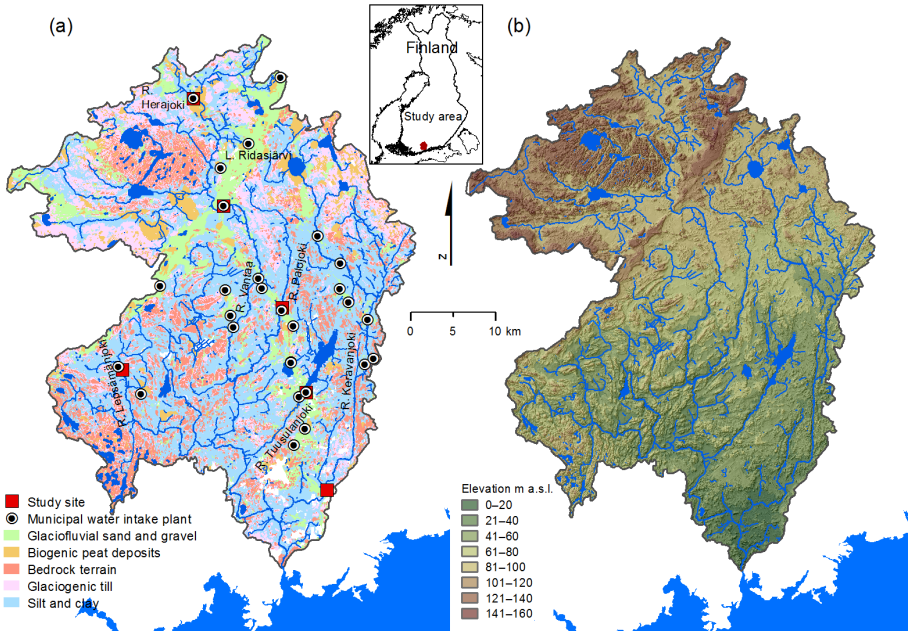

Figure 1. (a) Quaternary deposits and study sites in the River Vantaa catchment. **(b)** Elevation model of the River Vantaa catchment. (Basemap Database © National Land Survey of Finland 2010; Quaternary Deposit Database © Geological Survey of Finland 2008; Watershed Database © SYKE 2010; Topographic Database © National Land Survey of Finland 2010; Watershed Database © SYKE 2010).

HESSD
12, 2435–2476, 2015

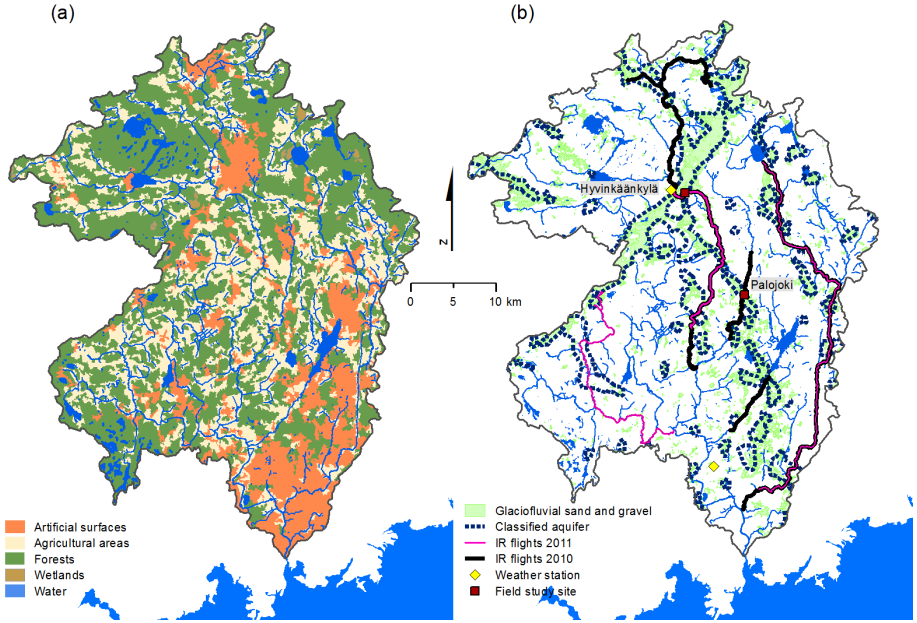

Figure 2. (a) Land use in the River Vantaa catchment. **(b)** AIR flights over the Rivers Vantaa, Herajoki, Palojoki, Keravanjoki, Tuusulanjoki and Lepsämänjoki in 2010 and 2011. (Corine land cover © National Land Survey of Finland 2010; Basemap Database © National Land Survey of Finland 2010; Quaternary Deposit Database © Geological Survey of Finland 2008; Groundwater Database © SYKE 2010; Watershed Database © SYKE 2010).

HESSD
12, 2435–2476, 2015

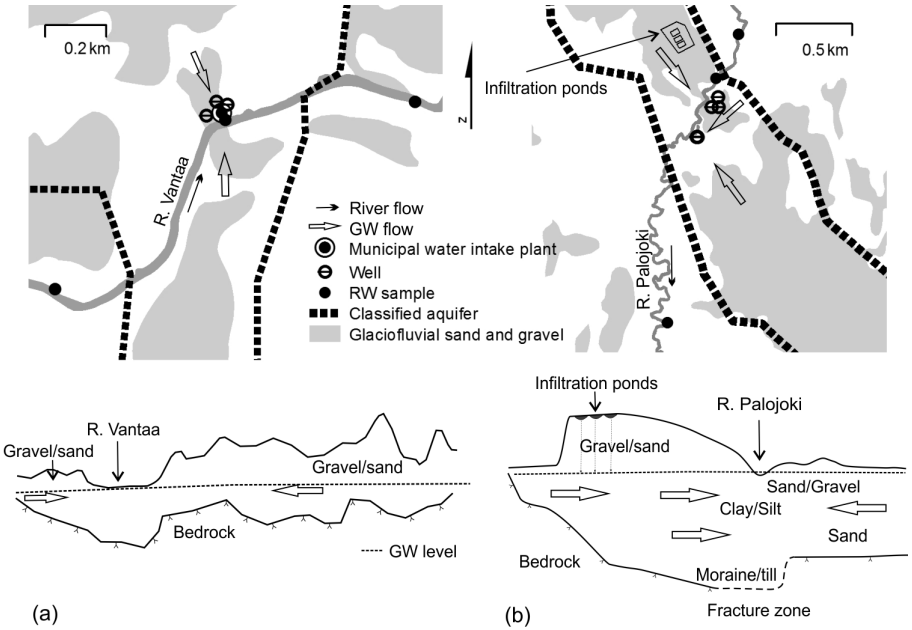

Figure 3. Schematic diagrams of the field study sites: **(a)** Hyvinkäänkylä field study site (bedrock elevation data from Breilin et al., 2004); and **(b)** River Palojoki field study sites (modified from Kortelainen and Karhu, 2006). (Basemap Database © National Land Survey of Finland 2010; Quaternary Deposit Database © Geological Survey of Finland 2008; Groundwater Database © SYKE 2010; Watershed Database © SYKE 2010).

HESSD
12, 2435–2476, 2015

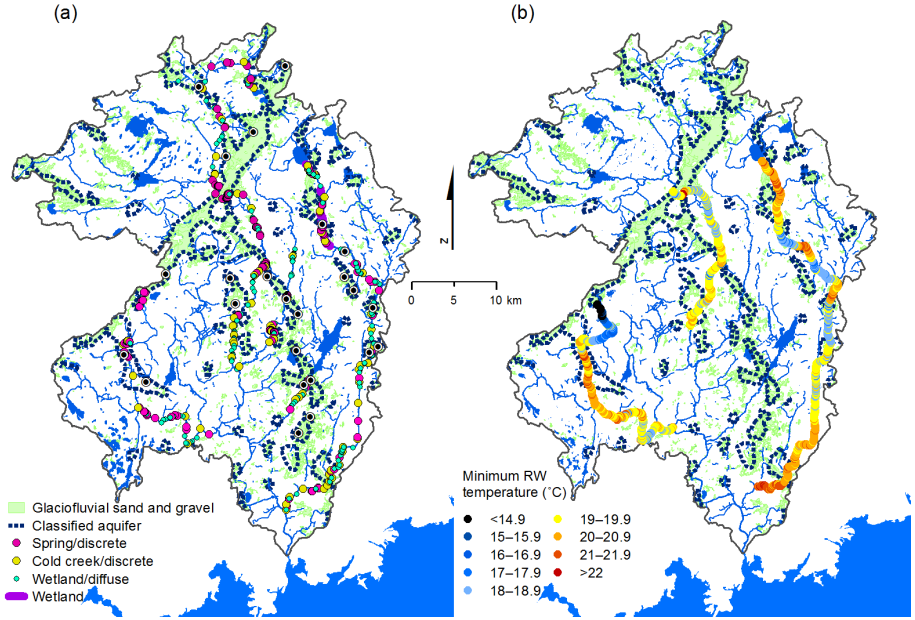

Figure 4. (a) Thermal anomalies identified in the AIR surveys in 2010 and 2011. **(b)** The longitudinal profiles of T_{minr} of the Rivers Vantaa, Keravanjoki and Lepsämänjoki in 2011 (Basemap Database © National Land Survey of Finland 2010; Quaternary Deposit Database © Geological Survey of Finland 2008; Groundwater Database © SYKE 2010; Watershed Database © SYKE 2010).

HESSD
12, 2435–2476, 2015

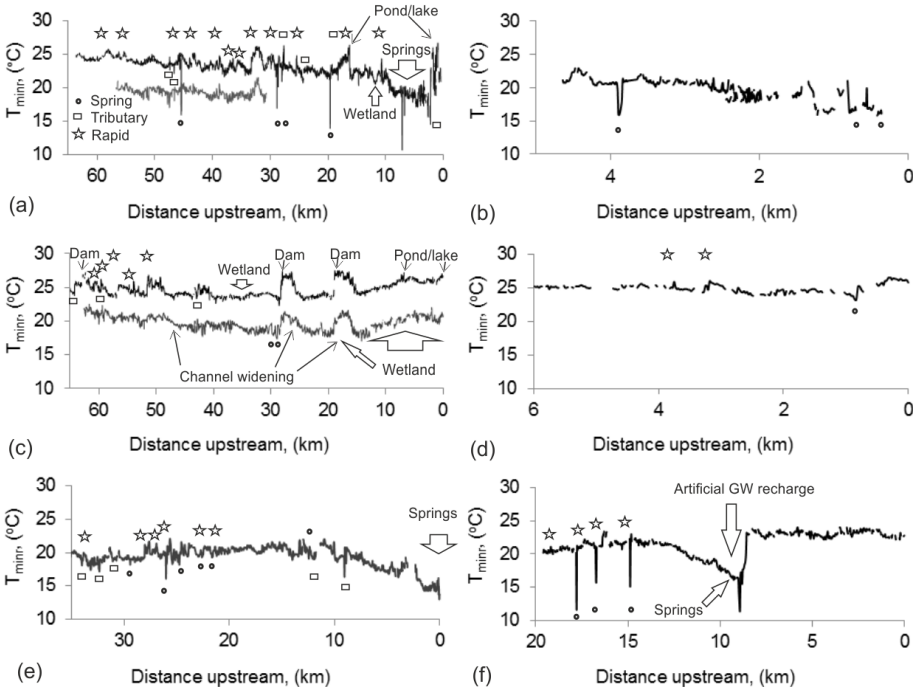

Figure 5. Longitudinal profiles of T_{minr} of the Rivers Vantaa **(a)**, Herajoki **(b)**, Keravanjoki **(c)**, Tuusulanjoki **(d)**, Lepsämänjoki **(e)** and Palojoki **(f)** in 2010 and 2011. Notable tributary confluences, GWSW exchange, dams, rapids and channel morphology changes are marked in profiles.

HESSD
12, 2435–2476, 2015

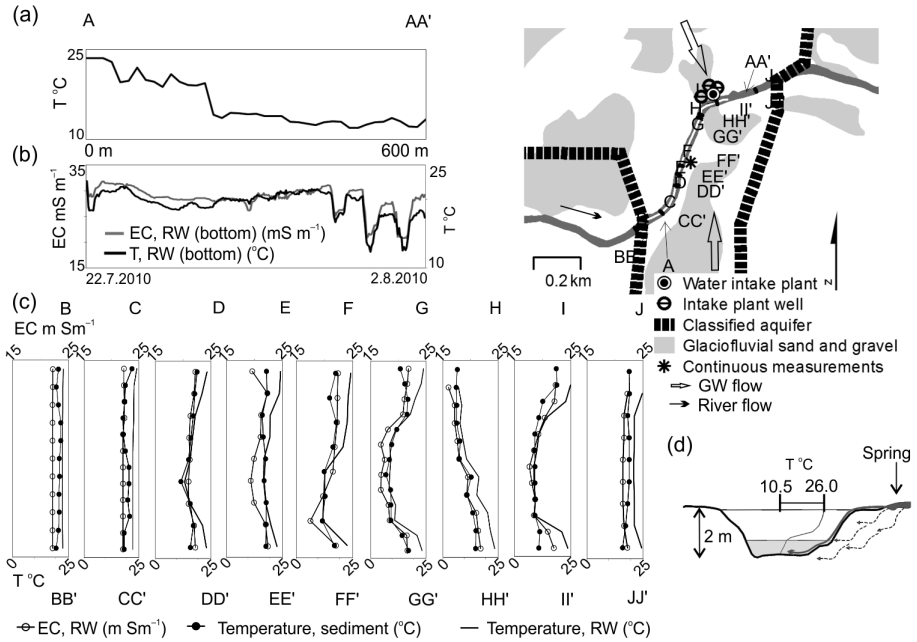

Figure 6. Field studies at the Hyvinkäänkylä study site in the low-flow period in July 2010: **(a)** longitudinal profile of RW temperatures (A–AA′) near the sediment–water interface; **(b)** continuous measurements of temperature and EC in RW 0.3 m above the river bottom (monitoring period from 22 July to 2 August 2010); **(c)** cross-sectional profiles (from B–BB′ to J–JJ′) of temperature and EC in RW near the sediment water interface and temperature in the sediment (water depth ranging from 0.10 to 2.0 m) and **(d)** schematic figure of stratification and the vertical RW temperature profile at cross-section F–FF′.

HESSD
12, 2435–2476, 2015

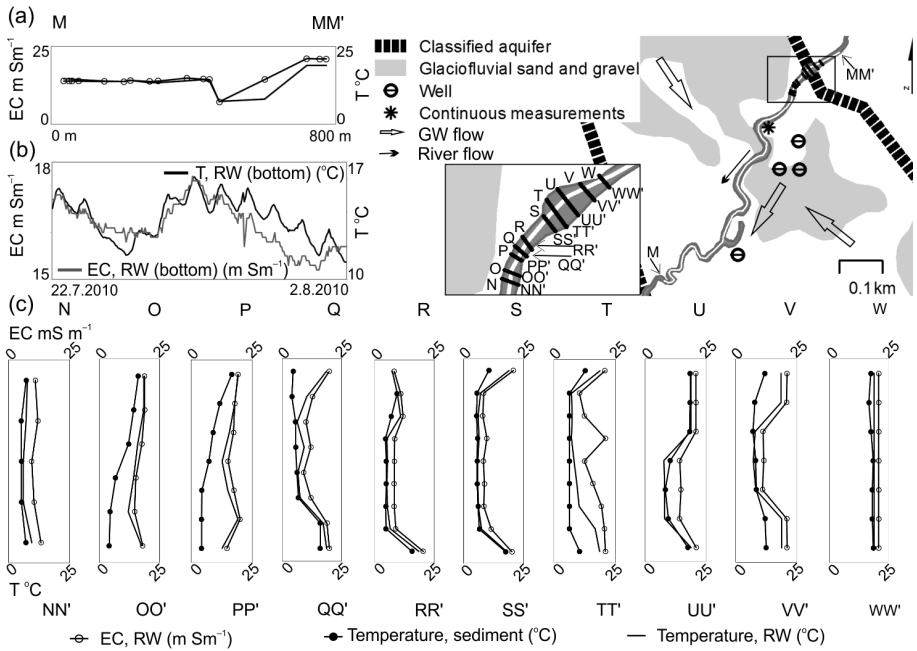

Figure 7. Field studies at the River Palojoki study site during the low-flow period in July 2010: **(a)** longitudinal profile of RW temperatures (M–MM′) near the sediment–water interface; **(b)** continuous measurements of temperature and EC in RW 0.2 m above the river bottom (monitoring period from 22 July to 2 August 2010) and **(c)** cross -sectional profiles (from N–NN′ to W–WW′) of temperature and EC in RW near the sediment–water interface and temperature in the sediment (water depth ranging from 0.10 to 1.62 m).

HESSD
12, 2435–2476, 2015

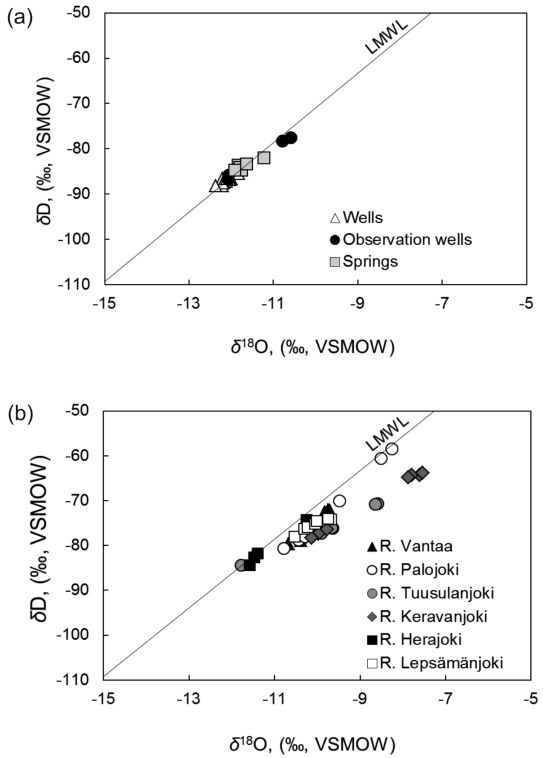

Figure 8. The $\delta^{18}O$ and δD values in the studied rivers: **(a)** the $\delta^{18}O$ and δD values of GW samples and **(b)** the $\delta^{18}O$, δD and DSi values of RW samples. The data are shown against the local meteoric water line (LMWL) ($\delta D = 7.67\ \delta^{18}O + 5.79$ ‰) defined by Kortelainen (2007).

HESSD
12, 2435–2476, 2015